

# We are IntechOpen, the world's leading publisher of Open Access books Built by scientists, for scientists

6,900

Open access books available

186,000

International authors and editors

200M

Downloads

Our authors are among the

154

Countries delivered to

TOP 1%

most cited scientists

12.2%

Contributors from top 500 universities



WEB OF SCIENCE™

Selection of our books indexed in the Book Citation Index  
in Web of Science™ Core Collection (BKCI)

Interested in publishing with us?  
Contact [book.department@intechopen.com](mailto:book.department@intechopen.com)

Numbers displayed above are based on latest data collected.  
For more information visit [www.intechopen.com](http://www.intechopen.com)



---

# Direct Electrolytic Al-Si Alloys (DEASA) – An Undercooled Alloy Self-Modified Structure and Mechanical Properties

---

Ruyao Wang and Weihua Lu

Additional information is available at the end of the chapter

<http://dx.doi.org/10.5772/52962>

---

## 1. Introduction

Aluminum became attractive only after the invention of Hall-Heroult electrolysis process in 1886. In the earlier part of last century, the usage of aluminum products was restricted in decorative parts. After World War II, a dramatic expansion of the aluminum casting industry occurred. Many new alloys were developed to comply with the engineering requirements. Among the commercial aluminum alloy castings, Al-Si alloy is the most commonly used and constitutes 85-90% of the total aluminum cast parts produced. Al-Si alloys containing silicon as the major alloying element offer excellent castability, good corrosion resistance and machinability. Small amounts of Cu, Mg, Mn, Zn and Ni are being added to achieve strengthening of Al-Si alloys.

Al-Si alloys have been made for a long time by simply adding crushed silicon metal or a high-silicon aluminum base master alloy to molten aluminum in reduction cell or smelting furnace. In those processes pure silicon and aluminum are needed, and both metals are reduced from oxides in electrolytic cell. The idea of direct electrolytic reduction of silica dissolved in the cryolite bath in electrolytic cell has been developed at the end of nineteenth century. The idea to produce alloys in electrolytic process is not new. For several years before Hall-process the Cowles process, by which Cu-Al alloys in range of 30-40% Al were directly reduced from a mixture of  $\text{Al}_2\text{O}_3$  and CuO or Cu by electric arc at high temperature, was used [1].

1891 Menit firstly conducted the experiment to reduce the silica to silicon metal in Hall cell. In 1911 Frilley [2] achieved the production of Al-Si alloys containing less than 5% silicon by direct electrolytic reduction of alumina-silica and 5-96% silicon by aluminum-thermal

reduction in laboratory. Frilley also obtained Mn-Si, Cr-Si, Fe-Si, Cu-Si and Si-Ni in electrolytic cells. Moreover, he found that the silicon appearance in Al-Si alloy with less than 10% Si was very fine and different from the existed alloy, but no attention had been paid on the change of structural characteristics of silicon due to limited usage of aluminum in industry at that time. Fridley's discovery revealed that electrolytic process is a powerful potential measure to improve the quality of alloy.

In the middle of last century a number of works had been reported to electrolyze Al-Si alloy in Hall cells, to which pure silica, quartzite containing more than 99% SiO<sub>2</sub> [3], sand stone with about 90% SiO<sub>2</sub> [4] glass scrap having 72% SiO<sub>2</sub> [5], bauxite with 11%SiO<sub>2</sub> [6], sand and clay [7] were added. Recently the refractories from spent potlining were successfully introduced to alumina reduction cells to produce Al-Si alloys [8]. As well known, the purity of molten aluminum is of major concern in electrolytic reduction process. The impurity is considered as a negative factor, deteriorating operation conditions. Hence, the direct electrolytic reduction of silica in Hall cell is a difficult process. There are two severe problems related with silica added into molten cryolite, in which silica must be easily dissolved. One of them is how to compensate for alumina generated by the reaction of aluminum with the added silica for achieving a desired chemical composition of alloy. Other is that direct addition of silica or other silicates often results in the formation of the heavy ridges of silicate along the bottom of the cell, as a result the cell becomes inoperable, so limiting the size and placement of the ridge is a major concern in production. In 1970s C. J. McMinin and A.T. Tabereaux [9, 10] provided a procedure to strictly control the feed of alumina and silica into the cell, stabilizing the electrolytic process and successfully producing Al-Si alloys with up to 16%Si in Hall cell. However, they viewed this process to be economical when the price of silicon greatly increases. Production of Al-Si alloys in electrolytic reduction cell had not found industrial application.

Since 1970s many works have been carried out on direct electrolytic production of Al-Si alloys(DEASA) in China [11]. Most Chinese bauxites contain high content of silica, titania and small amount of rare earth oxides. It is very difficult to extract the pure alumina from bauxite by the Bayer process [12]. In electrolytic process the charge is composed of bauxite, from which the iron oxide is removed, and alumina, using which to regulate the proportion of bauxite added into salt bath in terms of the desired chemical composition of Al-Si alloy. Note that bauxite tested is easily to be dissolved into molten electrolyte compared to the commercial bauxites. It would be an important factor to successfully produce Al-Si alloys in alumina reduction cells. At the end of last century several thousand tons of DEASA ingots containing Si content from 6% to 12% have been used in foundries to produce car parts such as engineering block and head, wheel and piston [12- 14]. Table 1 lists the chemical compositions of some DEASA ingots, which contain higher level of impurities such as Na, Sr, Ti and rare earth elements compared to commercial alloys. Undoubtedly it is related with bauxite composition. .

Since 1980s author has focused attention on the microstructure of DEASA and its mechanical properties [15]. It has been found that the microstructure and fracture surface of

DEASA ingots are very fine and similar to impurity-modified Al-Si alloy. Hence this phenomenon is characterized as self-modification due to no impurity- modifier added. The further research indicated that self-modification is attributed to the eutectic undercooling during solidification of DEASA. To answer the question why self-modified microstructure occurs and how it links with the electrolytic process, we must discuss some events related with electrolysis process. This chapter restricts the consideration into the structural characteristics of alloys and its original, which is related with electrolytic process. The details of electrolysis process can be referred to References [11,12 ].

| Alloy*       |            | Si    | Cu    | Mg    | Mn    | Ni    | Zn    | Fe   | Cr    | Ti   | Na      | RE     | Sr     |
|--------------|------------|-------|-------|-------|-------|-------|-------|------|-------|------|---------|--------|--------|
| EZL101       | top        | 7.9   | <0.01 | —     | 0.01  | <0.01 | 0.01  | 0.25 | <0.01 | 0.33 | —       | 0.002  | 0.001  |
|              | No1 bottom | 8.2   | <0.01 | —     | 0.01  | 0.01  | 0.01  | 0.24 | <0.01 | 0.35 | —       | 0.002  | 0.001  |
| EZL101 No2   |            | 7.3   | <0.01 | 0.36  | 0.01  | 0.02  | <0.01 | 0.11 | —     | 0.11 | <0.0001 | —      | 0.001  |
| ESi 9**      | No1        | 9.5   | <0.02 | 0.010 | 0.060 | 0.15  | 0.03  | 0.65 | 0.02  | 0.48 | 0.0045  | 0.038  | 0.0034 |
|              | No2        | 9.2   | <0.02 | 0.02  | 0.005 | 0.12  | 0.02  | 0.44 | 0.18  | 0.66 | 0.014   | 0.037  | 0.0026 |
| EZL102       |            | 12.2  | <0.01 | 0.15  | 0.005 | —     | <0.01 | 0.50 | —     | 0.12 | —       | —      | —      |
| ZL108        |            | 11.60 | 1.95  | 0.65  | 0.62  | 0.30  | —     | 0.25 | —     | 0.20 | 0.0020  | —      | 0.000  |
| EZL109       |            | 12.1  | <0.01 | 0.91  | 0.01  | 0.81  | <0.01 | 0.25 | —     | 0.09 | 0.0023  | —      | 0.000  |
| ZL101 (A356) |            | 6.7   | —     | 0.39  | 0.01  | 0.005 | —     | 0.06 | 0.016 | 0.12 | —       | 0.0005 | 0.002  |

E is abbreviation for electrolysis. ZL represents “cast aluminum alloy” in Chinese:

\* Alloy designations are to Chinese specification.

\*\* Alloy mark representing an electrolytic Al-9% Si-0.5%Ti alloy.

**Table 1.** Chemical analysis of DEASAs ingot wt%

## 2. Behavior of alloy melt in electrolytic process

The electrolysis cell runs at around 950°C with a voltage drop of 4.5-5.5 V across each cell[11]. The bauxite, from which iron oxide is removed, contains SiO<sub>2</sub>, TiO<sub>2</sub>, Fe<sub>2</sub>O<sub>3</sub>, Na<sub>2</sub>O, CaO and rare earth oxides (RExO<sub>y</sub>) ,besides the Al<sub>2</sub>O<sub>3</sub>. During electrolysis process those compounds are reduced to Al, Si, Ti, Fe, Na, Ca and RE, respectively, which in atomic form continuously remove from electrolyte to the carbon bottom of the pot, forming a homogeneous Al-Si alloy melt with several impurities, as shown in Tab.1. Then the melt is siphoned out of the reduction cell at 24h intervals and held in a 10 ton insulated metal-mixer for homogenizing the composition, then poured into ingot mould with dimension of 100×60 ×600mm<sup>3</sup> and weight of 10kg, without any impurity-addition or treatment. Hence, there are four factors i.e. homogeneous melt, superheating, impurity and electric field (current density and anode potential), influencing the structure of DEASA melt and its crystallographic characteristics and properties in solid state.

In many years a lot of studies have been done on the structure of liquid metals, including Al-Si alloy. The liquid metals can be considered as a system composed of ions and electrons, which are moving through the disordered liquid [16-18]. Below we discuss how superheating and electric field change the structure of Al-Si melt and its crystallization

### 2.1. Effect of superheating on the crystallographic characteristics of Al-Si alloys

As well known melt superheating is a powerful factor influencing the microstructure and properties of commercial Al-Si alloys. The effect of superheating is associated with the temperature, holding time and cooling rate during solidification [19-24]. In 1990s many researchers [21,25] investigated the regularity of variety of viscosity and density of family of Al-Si alloy in liquid state with temperature, revealing that as temperature exceeding about 1000°C, these physical properties dramatically change. Therefore, they suggested that for the near eutectic Al-Si alloy containing 10-14% Si there is a critical temperature in range of 1050-1150°C, as shown in Fig.1, above which the silicon grains and other heterogeneous substances such as iron-rich particles are dissolved in melt, resulting in a homogeneous melt, which will change the crystallographic characteristics of alloy. This event has been proved by recent studies. At the beginning of this century X.F. Bian et al studied Al-13%Si alloy melt heated in the temperature range of 625-1250°C using high temperature X-ray diffractometer [22] and reported that when increasing the temperature to 875°C a sudden change of the atomic density and the coordination number of the Al-13%Si alloy melt occurs, demonstrating that the liquid structure has changed, which is caused by dissolving of Si-Si clusters into aluminum melt. In other study it has been found that at the temperature of about 1050°C the electrical resistivity of hypereutectic Al-16%Si alloy melt steeply changed and hereditary effect of different original structure can be eliminated after remelting, indicating that the change of liquid structure happened at temperature of 1050°C[26]. Hence Al-Si alloy melt at high temperature consists of two ion groups: Al-Si and Si-Si groups, which appear to consolidate the short-range order and the electrons are moving through the disordered melt [27-29]. Based on the experimental results P.J.Li [23] considered that in homogeneous Al-Si alloy melt the size of Si-Si and Al-Si micro-heterogeneous clusters range is from 10 to 100Å. M. Singh reported that in Al-Si alloys either hypoeutectic or hypereutectic silicon is present as silicon cluster essentially with the size of about 50-70 Å [27]. Moreover, as increasing the temperature, the size and number of ion groups simultaneously decrease.

P.C. Popel et al [21, 23] studied the influence of superheating on the crystallographic characteristics of alloys and revealed that superheating Al-Si alloy shifts its eutectic reaction toward higher level of silicon accompanying with the appearance of Al-dendrite. As temperature is higher than 780°C, eutectic silicon becomes finer with the fine  $\alpha$ -Al dendrite. When heating temperature is in range of 900-1000°C, the size of silicon flake is less than 7 $\mu$ m. It is interesting that heating at temperature higher than 1000°C the modified silicon appears in eutectic alloy. The heating at 1000°C is capable of eliminating the occurrence of primary silicon and refining  $\alpha$ -Al dendrite in Al-17%Si alloy. But when superheating hypereutectic Al-20%Si alloys at 950°C the primary silicon particles become finer [24, 30]. The higher the temperature, the finer the silicon grain. It would be expected that a higher

superheating temperature is required for hypereutectic Al-Si alloys having higher silicon content to achieve a complete eutectic structure. It is worthy of note that if the holding time is insufficient to dissolve all the silicon particles present in original alloy, even the superheating at 1200°C does not significantly change the crystallographic characteristics of alloy, and the modified structure does not appear [31].

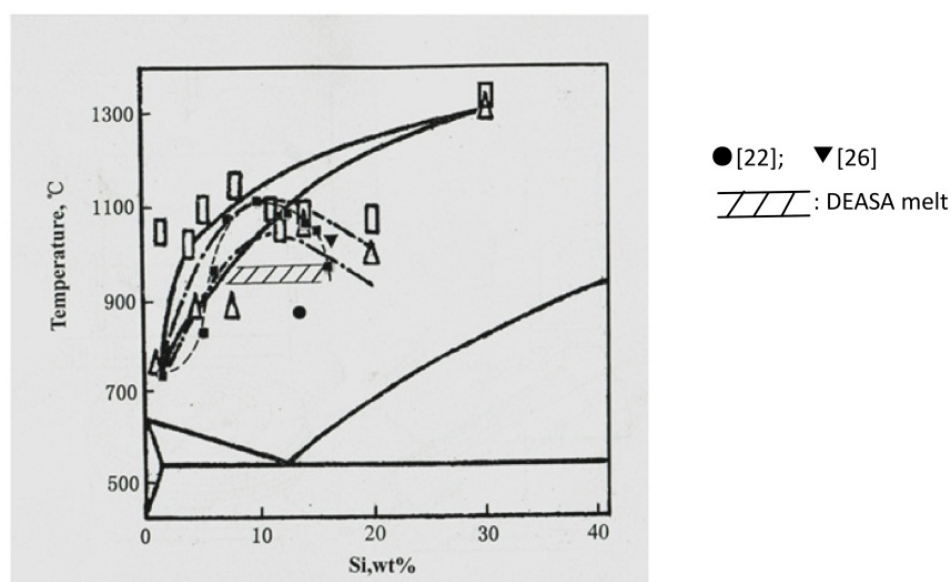


**Figure 1.** The dome of decay of metastable colloidal microheterogeneity in Al-Si melts [21,23]

For hypoeutectic alloys as temperature rises to 950°C the dendrite arm spacing(DAS) steeply decreased and the dislocation density in  $\alpha$ -Al dendrite increased. Moreover, the eutectic silicon tended to a fine fibrous structure [32].

Overheating significantly increases the content of silicon, magnesium and iron in  $\alpha$ -Al-dendrite in hypoeutectic alloy [33]. As overheating Al-8%Si alloy at temperature of 950°C for 10min silicon and magnesium content solved in  $\alpha$ -Al-dendrite increases to 1.9% and 0.3%, respectively, much higher than their solubility in Al-matrix at room temperature. Undoubtedly, overheating is one of the factors strengthening the mechanical properties of alloys.

Superheating also prompts the morphological variety in iron-bearing compound in alloys [34]. As heating Al-7%Si-Mg alloy at temperature higher than 800°C, AlSiFe compound appeared in Chinese script form instead of coarse needle-like shape, increasing the impact strength of alloy. It is apparent that superheating is a powerful mean greatly affecting the feature of microstructure in Al-Si alloys.

It is worth noting that the overheating effects on the change in structure significantly depends upon the cooling rate in freezing in alloy [23, 35]. For hypereutectic Al-17%Si alloy even heated at temperature in the range of 1000-1050°C the primary silicon grows faceted in sand castings, where the freezing rate is less than 10°C/sec. By contrast the formation of



more equiaxed, nearly globular silicon crystal can be observed if the melt is quenched with the cooling rate of higher than  $100^{\circ}\text{C}/\text{sec}$ .

The reason why superheating leads to a change in crystallographic characteristics of alloys is associated with the undercooling generated by a variety of structure in molten alloy, where the size and number of Si-Si clusters acting as a nuclei of eutectic silicon in solidification of alloy greatly affect the crystallization of alloy[36]. Higher superheating decreases Si-Si cluster in size and amount, depressing the liquid-to-solid transition temperature, as a result a deep undercooling occurs. A.Y.Gubinko[37] reported that superheating an Al-Si alloy melt to  $100^{\circ}\text{C}$  above its liquidus temperature offers an undercooling twice as great as for a melt superheated  $35^{\circ}\text{C}$ . The higher the superheating temperature, the greater the undercooling in freeze of alloy. Note that temperature in electrolysis cell is about  $950^{\circ}\text{C}$  lower than the critical temperature, above which structure of melt transits from microheterogeneous to homogeneous state (Fig.1) and DEASA is intrinsically homogeneous due to its reduction from oxides. Hence, it would be thought that the overheating in reduction cell does not affect the structure of melt, but holding DEASA melt in metal-mixer for long time causes the structural transition from homogeneous to heterogeneous state in some degree.

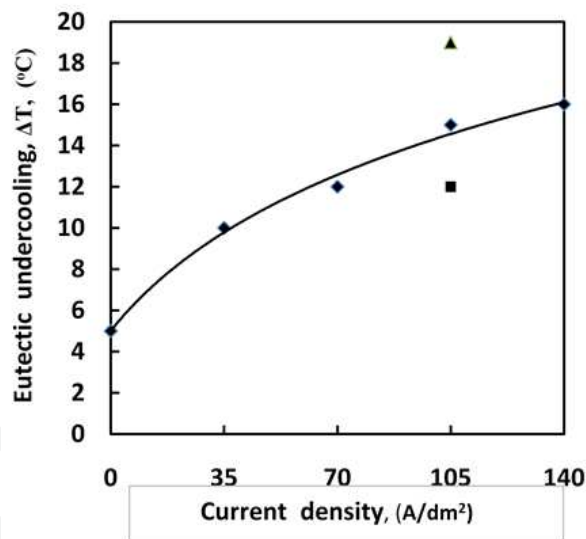
## 2.2. Role of electric field in the crystallization of Al-Si alloys

Over the past decades a lot of studies relating with the effect of electric field on the structure and properties of Al-alloys have been carried out [38-42]. Electric field either continuous current or pulse electric discharge deeply affects crystallographic character of alloy and its properties. In this chapter we will only focus our attention on the effect of direct current, which is related with electrolysis process.

By introducing the direct current into molten Al-10%Si alloy at  $740^{\circ}\text{C}$  for treating time of 50min, H.Li et al studied the effect of different current density on the structure and mechanical properties of alloy [43]. It was found that the electric field causes a morphological transition of eutectic silicon from flake to fibrous shape, accompanying with the reduction of second  $\alpha$ -Al dendrite space. As increasing the electric current density to  $30\text{A}/\text{dm}^2$  silicon phase grows modified and finally primary Al-dendrite appears in near-nodular shape. As a result the elongation of alloy was raised by 100% and its tensile strength was improved by 15%. It is interesting that an increase in current density leads a rise in undercooling in freezing of alloy as shown in Fig.2. When increasing current density to  $100\text{A}/\text{dm}^2$  a deep undercooling of  $15^{\circ}\text{C}$  occurs, then undercooling grows slowly with current density. Undoubtedly, the deep undercooling is the reason of the change in morphology of silicon particles.

L. G. Huang et al introduced direct-current into melt poured into mould during solidification and investigated the effect of current density on the structural feature of Al-4%Si and Al-10%Si alloys, which were firstly heated at  $700^{\circ}\text{C}$ . It was found that silicon became finer with direct-current density and reached a limit as the density is increased to  $283\text{A}/\text{dm}^2$  and the size of  $\alpha$ -Al dendrite arm space (DAS) also reduced with a minimum at

density of 325A/dm<sup>2</sup>. It is interesting that the effect of alternating current is the same to direct- current [44]. B.A. Timchenko et al [45, 46] studied the effect of high direct-current density (100-10 000A/dm<sup>2</sup>) on the quality of casting made of eutectic Al-12%Si alloy. When a large current is passed through alloy during its solidification, the solubility of silicon in  $\alpha$ -Al matrix is raised to 20%, and its distribution becomes more homogeneous with a reduced size of silicon particles. In addition, the mold filling ability (fluidity) of casting alloys is greatly improved accompanying with a less tendency to gas porosity and shrinkage. As a result the tensile strength and hardness are increased by 10%. Recently A. Prodhon [47] reported that molten eutectic Al-12.16%Si alloy, which firstly was superheated to 750°C, can be degassed by direct- current treatment during solidification (semisolid state). The initial hydrogen level in alloy made from the ingot is about 2.5ppm, and under current treatment within 10min the hydrogen content is reduced to near 1.7ppm, which is necessary for producing a casting without porosity [47]. However, a large current density will cause an increase of hydrogen concentration. It is obvious that electric field, which is introduced into melt at more or less higher temperature or during solidification, improves the casting properties with an increase in mechanical index. This is attributed to the structural rearrangement of alloy melt generated by electric field. However, we are unable to clarify how the electric field affects the properties of DEASA melt due to the absence of experimental results at high temperature of above 900°C.



◆[22]; ■EZL101; ▲EZL109

**Figure 2.** Eutectic undercooling in freezing against current density in Al-Si melt.

The major effects induced by electric field on the behavior of alloy melt include Joule's effect and electron-transport. Electric current causes the input of heat due to Joule's heating effect, which leads to an increase in solidification time, resulting in the improvement of fluidity of alloy, and hence the reduce of shrinkage and porosity[47]. Obviously, Joule's heating effect doesn't affect the properties of DEASAs, which solidify without electric field in present study.



In electrolysis process Al-Si alloy melt is ionized to macroscopic homogeneous  $\text{Al}^{3+}$  and  $\text{Si}^{4+}$  ions, and conduct electrons, which are moving through the melt. Under electric potential, positive ions migrate to the cathode and the electrons move toward the anode. The so-called electron-transport, which depends on ionization potential of constituent elements and its mobility in the applied field, is most important factor that reduces the solute distribution coefficient and influences the rearrangement of elements on the solid-liquid alloy boundary during solidification, therefore reducing the constitutional undercooling and changing the crystallographic behavior of alloys. Under the current potential, the conduction electrons surrounding the aggregates of Si<sup>+</sup>-rich or Al<sup>+</sup>-rich groups are readily to be transferred to unlike atoms, making the groups unstable [17,28]. When the electron-drag applied to the ions, the unstable groups either Si<sup>+</sup>-rich or Al<sup>+</sup>-rich are capable of splitting into smaller one. The smaller Si<sup>+</sup>-rich aggregators, which act as a nuclear center of silicon phase in Al-Si alloys as reported in reference [36] will promote a larger undercooling in eutectic reaction, which strongly change the crystallographic characteristic of silicon phase. Our data showed that compared to commercial unmodified Al-Si alloys eutectic arrest temperature in DEASA ingot drops to about 15-18°C [15], which is sufficient to modify the microstructure of Al-Si alloys either eutectic [48] or hypereutectic.

Summarizing the experimental results in literatures mentioned above, it is apparent that the effect of overheating on the microstructure and properties of Al-Si alloys is more or less same as electric current that leads the same variety in arrangement of melt in some degree, resulting in a large undercooling in solidification of alloy. It is worth noting that the structure of liquid DEASA is homogeneous in electrolysis process, and therefore, the effect of both of superheating and current field is weakened compared to the existing alloys. It is thought that in the electrolysis process the combination of both factors (superheating and electric field) provides Al-Si alloys a circumstance, where the ability of melt to stabilize the homogeneous structure is enhanced, hence the morphological transition of constituents of DEASA easily undergoes either under lower cooling rate during solidification or upon remelting compared to the common alloy. DEASA is an excellent undercooled alloy, of which the crystallographic behavior is same to alloy treated with electric field at high temperature and rapid cooling rate during solidification. This inference has been evidenced in present and previous studies [14,15, 49].

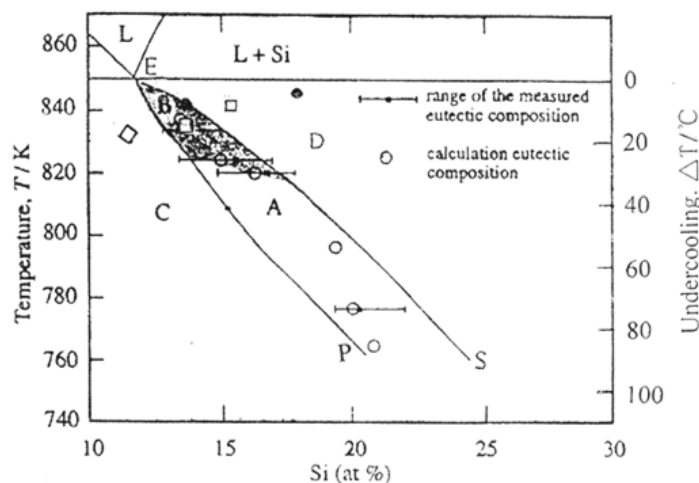
### **3. Crystallization feature of DEASA**

#### **3.1. Morphology of silicon phase and its inheritance upon remelting**

As well known, silicon is the major alloying element in Al-Si alloys and its morphology is primary important factor affecting the mechanical properties, castability, machinability and other physical properties. In 1950s it has been found that for Al-Si alloy the growth of silicon crystal is temperature-dependent and dictated by the undercooling in freezing [50]. Since then a number of investigations have been done to clarify the relationship between its morphology and undercooling in solidification [48,51-53]. In general, an eutectic

temperature undercooling of 6-8°C is necessary for appropriate modification for hypoeutectic or eutectic Al-Si alloys. If the combination of undercooling induced by cooling rate during solidification and modifier is below the critical value, an unmodified structure is obtained.

The relationship between temperature / undercooling in freezing and morphological transition including eutectic, primary silicon and aluminum phase in Al-Si alloys containing different silicon content can be described in quasi-equilibrium Al-Si diagram (Fig.3.)[54].



A,B: Quasi-eutectic zone; C:Al-dendrite + eutectic; D:Primary silicon + eutectic;

◇: Al-dendritic + eutectic in present work;

□: Coupled eutectic in present work;

●: Primary Si + eutectic in present work.

**Figure 3.** Quasi-eutectic zone in the Al-Si system.[54]

Compared to equilibrium diagram, where eutectic reaction runs at a constant temperature and silicon content, the region of formation of quasieutectic structure exists, i.e. in a wide range of temperature/undercooling and silicon content the eutectic structure can be observed. For hypereutectic Al-Si alloys with an increase in silicon content the region shifts towards higher silicon concentration and depresses the eutectic temperature, implying that a higher undercooling is required to produce quasieutectic structure and, meanwhile, the silicon content in quasieutectic is much more than equilibrium. Whether hypereutectic alloy displays a quasieutectic structure or quasieutectic plus primary silicon grain depends upon undercooling. Obviously, the microstructure of eutectic alloy composes of eutectic plus primary  $\alpha$ -Al dendrite in casting condition. On the other hand for hypoeutectic alloys due to eutectic shift toward higher silicon content the volume fraction of primary aluminum dendrite increases compared to the equilibrium Al-Si diagram with same silicon content, whereas with undercooling the volume fraction of Al-dendrite increases. In general, using the quasi-diagram the variety in crystallographic feature of Al-Si alloy with different silicon level and undercooling / temperature can be clearly explained.

In order to reveal this relationship between the crystallographic feature in DEASA and undercooling in freezing we observed the microstructure of DEASAs containing silicon content in the range 6- 18% and measured their cooling curves during solidification. Chemical analysis is listed in Table 1 and 2. The samples of eutectic (EZL102, EZL108 and EZL109) and hypoeutectic (EZL101 and ES9) alloys were cut from the center ingots. Hypereutectic alloys (EZL14, EZL16 and EZL18), of which the charge was composed of DEASA (EZL108)(Tab. 2.) ingot and Al-30%Si master alloy along with other master alloy additions., were melted in a 2 kg graphite crucible in an electric resistance furnace and heated to 850°C. After melting (Note: it is 1<sup>st</sup> remelting for EZL108) the molten alloy was held for 15 min to homogenizing the composition, then poured into a metallic mold, preheated to 250°C to form a casting 40x50x120mm<sup>3</sup> as shown in Fig.4. Pouring temperature is about 740°C for all alloys tested.

All tested alloys with different silicon content were repeatedly remelted to produce the unmodified structure with measured undercooling. This promotes to reveal the effect of undercooling on the structure in DEASA. Metallographic specimens were cut from the interiors of the casting near the site of a chromel-alumel thermocouple (Fig.4), by which the cooling curve was recorded. The cooling rate during solidification was about 1.0°C/sec.

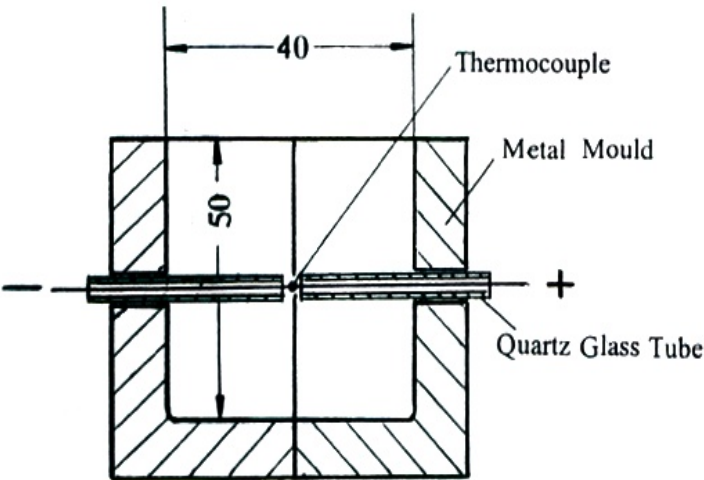


Figure 4. Mold and thermocouple

| Alloy  | Si    | Mg   | Cu   | Mn   | Ni    | Fe   | Ti   | Sr      | Ca     | Zr     | Remark    |
|--------|-------|------|------|------|-------|------|------|---------|--------|--------|-----------|
| EZL108 | 11.60 | 0.65 | 1.00 | 0.60 | 0.25  | 0.25 | 0.10 | <0.000  | 0.001  | 0.0070 | DEASA     |
| EZL14  | 13.70 | 0.55 | 0.80 | 0.31 | <0.05 | 0.25 | 0.03 | <0.0006 | <0.001 | 0.0010 | D*+AS30** |
| EZL16  | 15.70 | 0.59 | 1.00 | 0.34 | <0.02 | 0.35 | 0.03 | 0.0006  | 0.001  | 0.0072 | D+AS30    |
| EZL18  | 17.60 | 0.39 | 0.75 | 0.25 | <0.05 | 0.35 | 0.04 | <0.0006 | <0.001 | 0.0017 | D+AS30    |

D: DEASA; AS50: Al-30%Si master alloy.

Table 2. Chemical Analysis of DEASA tested

As well known, the alloying elements such as Mg, Cu, Mn, Ni, Fe and Zn lower the eutectic arrest temperature,  $T_E$ , in Al-Si alloy [55-57]. In general the following equation (1) is used to estimate the change of  $T_E$  in commercial alloys where the total of %Al +%Si is high, near 99% [57, 58].

$$T_E = 577 - (12.5 / \%Si) \left[ \begin{array}{l} 4.43 (\%Mg) + 1.43 (\%Fe) + 1.93 (\%Cu) + 1.7 (\%Zn) \\ + 3.0 (\%Mn) + 4.0 (\%Ni) \end{array} \right] \quad (1)$$

In present work the estimated eutectic arrest temperatures,  $T_{E,}$  range from 569°C to 573 °C depending upon the composition of alloys tested. Thus the undercooling,  $\Delta T$ , will be

$$\Delta T = T_E - T_E' \quad (2)$$

where  $T_E'$  is the measured eutectic temperature for given alloy.

Microstructure of eutectic DEASA (EZL102, EZL108 and EZL109) ingot is shown in Fig.5-8. A high volume proportion, 43-50%, of primary aluminum dendrite, which distributes evenly in modified eutectic matrix, can be found. and the eutectic undercooling is higher than 18°C that is significant different from the commercial eutectic alloy and similar to the impurity-modified alloys although the silicon content is just near to the eutectic composition.

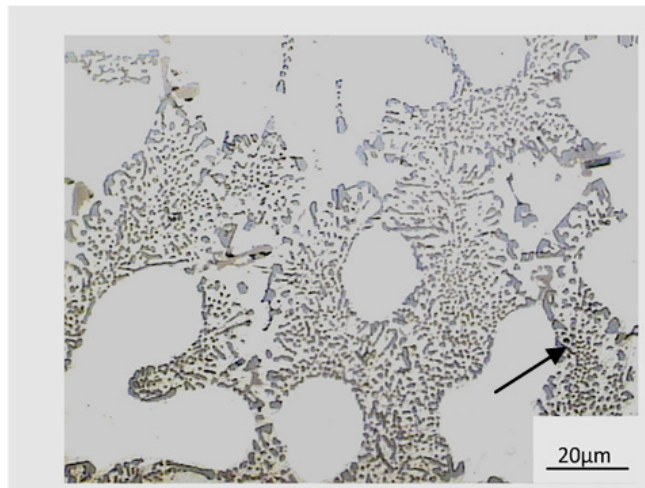


**Figure 5.** Optical micrograph of EZL102 ingot, showing as-cast self-modified structure. A few iron-rich crystal appears as a fine flake form as indicated by arrow.

The DEASA hypereutectic alloys, which contain 14% and 16%Si solidify with a completely modified eutectic microstructure (Fig.9 and 10) with undercooling of 12°C and 9°C, respectively. For the alloys with silicon content more than 17% (EZL18) the microstructure exhibits the coarse primary silicon crystals well distributed throughout the unmodified matrix as seen in Fig.11. In this case the eutectic temperature reached 568°C with undercooling of 5°C. In the hypoeutectic electrolytic Al-7%Si ingot the volume proportion of  $\alpha$ -Al dendrite reach 72% accompanying with modified eutectic silicon phase and undercooling of 12°C similar to



Sr-or Na-modified Al-7%Si alloy (Fig.12). As increasing silicon level to 9% the fine silicon grows in modified mode with a high volume percentage of  $\alpha$ -Al dendrite of 60% (Fig.13).

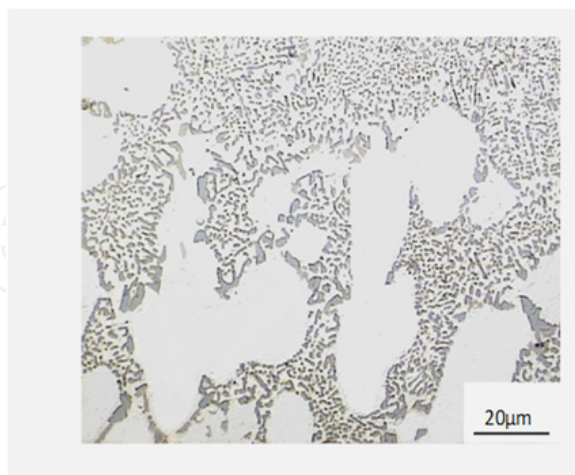


**Figure 6.** As-cast micrograph of EZL108 ingot, revealing self-modified structure. Optical

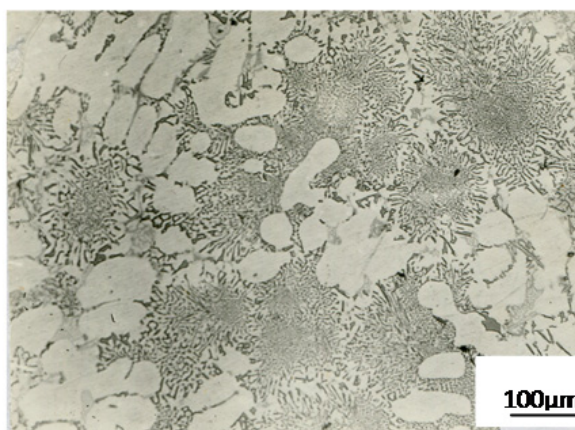


**Figure 7.** Microstructure in the top region of the electrolytic EZL109 ingot. The equiaxed coarse Al-Si eutectic cell appears, in which silicon grows in modification manner. Optical

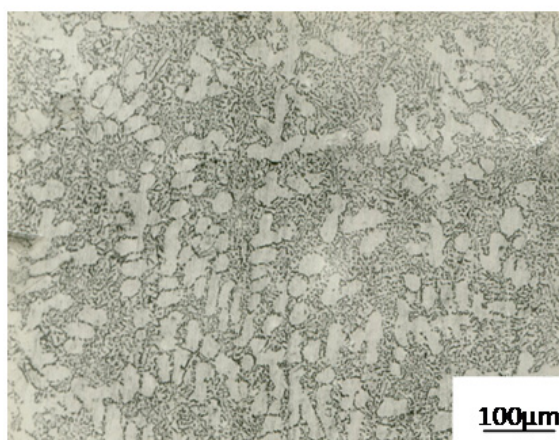


**Figure 8.** Optical micrograph in the bottom part of electrolytic EZL 109 ingot, indicating the fine self-modified structure.

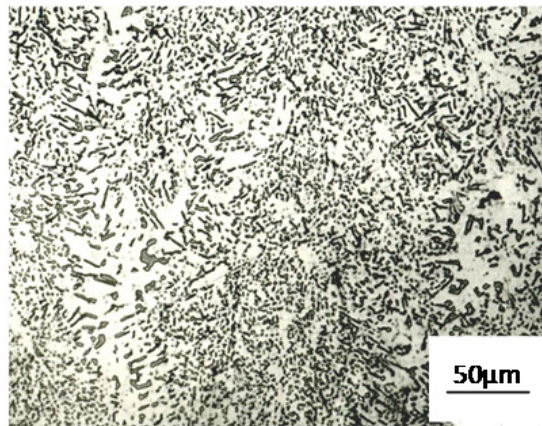


**Figure 9.** Self-modified microstructure of hypereutectic DEASA(EZL14), showing complete eutectic structure. On the boundary of eutectic cell some silicon flake can be observed. Optical.

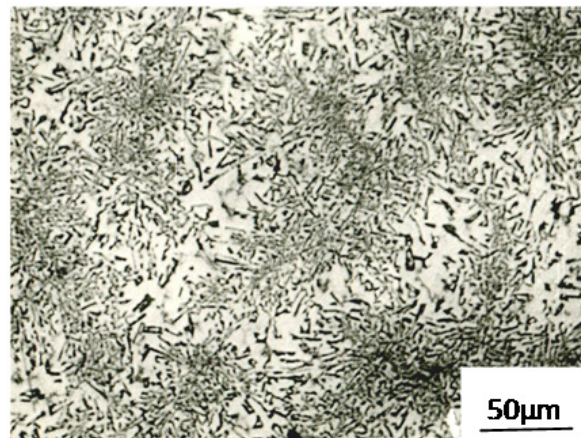


**Figure 10.** Optical self-modified structure of hypereutectic DEASA (EZL16). Complete eutectic structure appears accompanying some fine silicon flake on the boundary of eutectic cell.

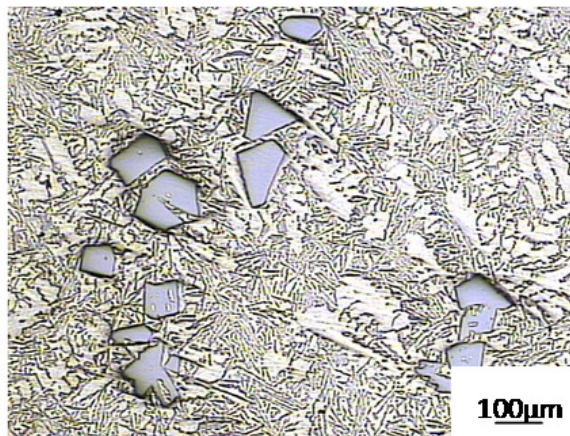


**Figure 11.** Microstructure of hypereutectic DEASA (EZL18). Coarse primary silicon distributes through the unmodified eutectic matrix. Some  $\alpha$ -Al dendrites occur. Optical

By combining with the regularity of morphological transition of silicon phase in Al-Si alloys treated by electric field at high temperature in literatures and our experimental results it



would be expected that the variety in crystallographic feature is attributed to the undercooling in freezing. This inference has been strongly supported by the experimental results in remelting DEASAs. The very fine self-modified structure in DEASA such as EZL101 and EZL109 is fully inherited upon first remelting with a deep undercooling of 9°C and 13°C, respectively, as shown in Fig.14. As undercooling is higher than critical value of 6-8°C, the alloys solidify in modified manner. In contrast, an unmodified structure in Al-17%Si alloy appears due to lower undercooling of 5°C

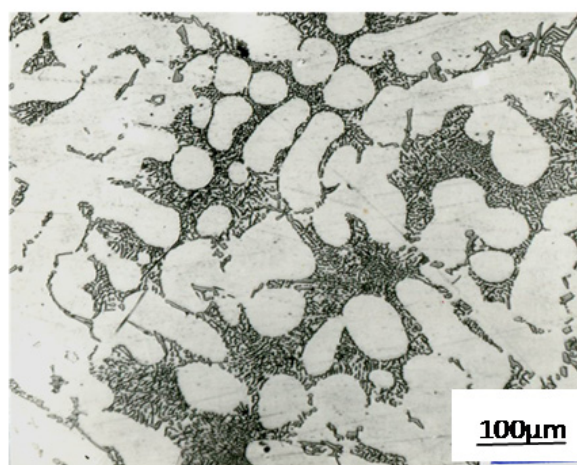


**Figure 12.** Microstructure of hypoeutectic DEASA(EZL101) ingot, demonstrating the self-modified structure with high volume fraction of  $\alpha$ -Al dendrite. Optical.

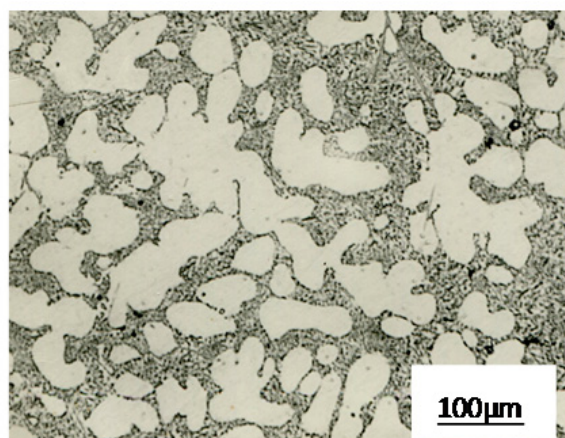
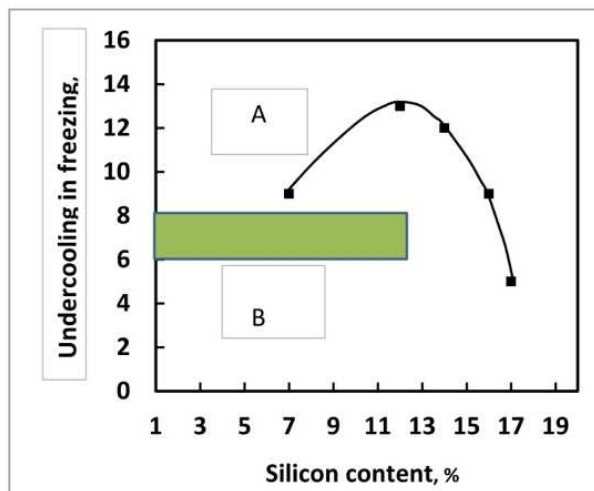


**Figure 13.** Optical micrograph of hypoeutectic DEASA(ES9) ingot, showing fine modified silicon phase with high volume percentage of  $\alpha$ -Al dendrite.

It is interesting that the modified structure in EZL109 fades considerably slower and even upon 3-fold remelting the modified structure is inherited (Fig15) with an undercooling of 5°C. However, for EZL101 with 7% Si or EZL102 having 12%Si after 3-fold remelting some silicon flake can be observed, displaying a decreased undercooling (Fig.16). It is thought that the alloying elements such as Cu, Mn, Ni and Mg prompt the occurrence of deep undercooling, strengthening the structural inheritance in EZL108, EZL109 and ES9 (Table I). In general, with 4-fold or more remelting the almost fully structural fading occurs and the

undercooling disappears. In this case the microstructure in eutectic EZL108 and EZL10 is composed of eutectic with few, if any,  $\alpha$ -Al dendrites. Note that upon first remelting the quasi-eutectic in DEASA hypereutectic alloys is subjected to fully fading, resulting in an appearance of coarse primary silicon grain distributed in unmodified eutectic matrix as shown in Fig.17, while the undercooling cannot be found. Fig.18 shows the variety of undercooling with remelting for DEASA (EZL101, EZL109). When undercooling is lower than 5°C, the inheritance of self-modified structure of EZL101 is subjected to significantly fading. In contrast, as undercooling decreases to 5°C the self-modified microstructure of EZL109 remains unchanged. Thus, it is reasonable to consider that for hypoeutectic and eutectic DEASAs the critical undercooling is 5°C, which is lower than critical value of 6-8°C for commercial Al-Si alloys. This phenomenon is thought to be associated with the homogeneous characteristics of DEASA melt, which cause silicon to solidify in modification mode at lower undercooling and cooling rate [23].



A: modified silicon B: unmodified silicon

 Critical region

**Figure 14.** Relationship between eutectic undercooling and Si content in remelted DEASA.

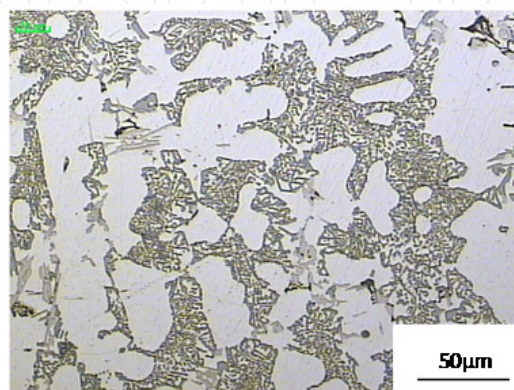


**Figure 15.** Optical structure of DEASA(EZL109) upon 3-fold remelting. Self-modified structure is fully inherited.

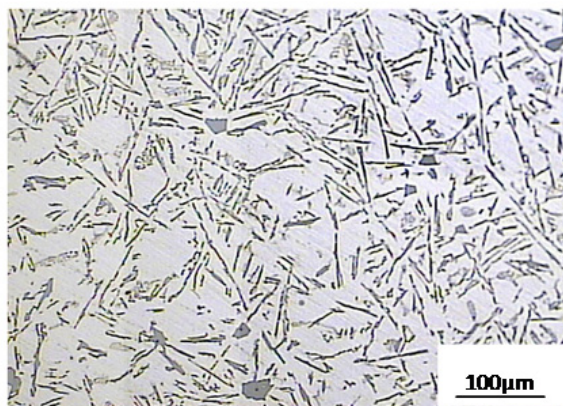


**Figure 16.** Microstructure of DEASA(EZL102) upon 3-fold remelting composed of unmodified structure. Some small faceted primary silicon appears. Optical.

It is worth noting that the self-modified structure is relatively insensitive to cooling rate as compared to commercial alloy. In general, the microstructure in top area of commercial ingot, where the cooling rate is very slow, displays coarse unmodified silicon flake but in the edge the fine silicon structure can be observed due to rapid cooling rate. Our observation reveals that there is no obvious difference in fineness of the eutectic between top and edge of eutectic DEASA ingot (EZL109) (Fig.7 and 8). It is expected to be associated with the homogeneous melt, of which the stability is strengthened by the electric field in electrolytic process. That would be thought to be superiority over commercial alloy to produce complex castings.

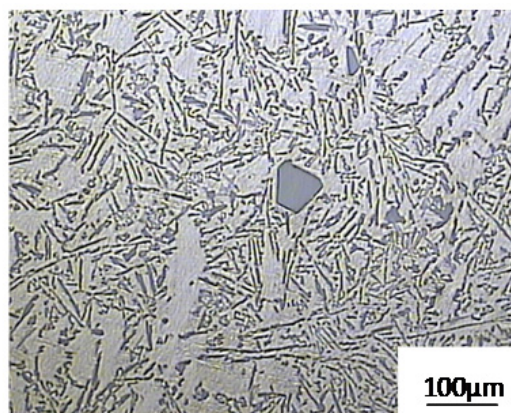


**Figure 17.** Optical micrograph of DEASA(EZL14) after first remelting. Self-modification is fully subjected to fading. Faceted primary silicon occurs

The origin of the variety of undercooling of DEASA is associated with the homogeneous character of its melt. The original DEASA melt either hypoeutectic or eutectic is intrinsic homogeneous, causing silicon to solidify at a large undercooling due to the lack of large silicon-rich clusters acting as nuclei in freezing. The repeated re-melting of DEASA, in which the large undissolved silicon particles exist, causes a lower undercooling, accompanying with the fading of modified microstructure. The homogeneous character in hypereutectic DEASA melting can be partially survives or fully lost depending upon the

silicon composition, because with increasing silicon content the undissolved silicon particles dramatically increases, nucleating silicon in solidification with a lower undercooling.

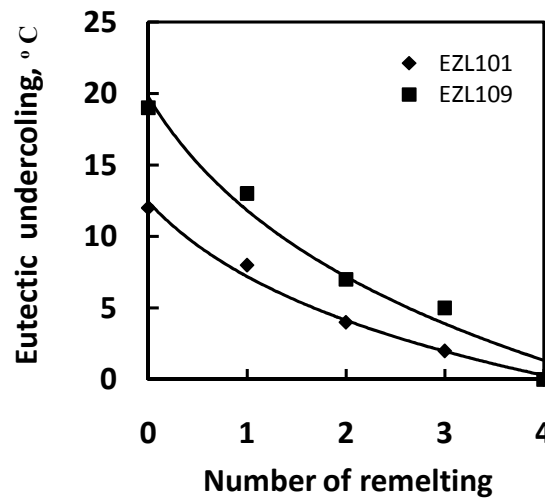


**Figure 18.** Relationship between undercooling and remelting undercooling and remelting

By combining the results in present and previous works we suggested the following growth mechanism of quasi-eutectic structure [49]. At initiation of the growth the silicon particle as nucleus would be assumed to be a nodule or irregular shape, with many different facets exposed in the melt [59-61]. Whether or not such a nucleus grows as polyhedron primary silicon crystal in freezing is determined by the degree of undercooling. As the nucleus grows, the boundary layer of eutectic composition starts to form around the growing nucleus and isolates it from the melting, thus preventing the further development of nucleus. With lower undercooling or higher silicon concentration the silicon atoms are capable of diffusing cross the layer to be trapped on the surface of the silicon nucleus, thus the silicon nucleus further grows, developing a primary silicon crystal and eutectic structure before the temperature of melt lowers down to the critical value shown by curve ES in Fig.3. Under high undercooling silicon atoms diffusion is limited, suppressing the primary silicon crystal to form. If the primary silicon cannot develop until the melt is cooled, reaching through the apparent eutectic temperature as curve ES shown in Fig.3, the quasi-eutectic structure occurs. In this case the silicon particles could act as the nucleus of eutectic, promoting the growth of eutectic structure.

As well known, whether the eutectic silicon grows in modified manner is attributed to the undercooling in solidification of alloy. This phenomenon is related with the entropy of melting and crystallographic structure as reported by A. Jackson in 1958 [62]. This relationship can be expressed as:

$$\alpha = (\Delta S / R) (N_s / N_v) \quad (3)$$

where  $\alpha$  is Jackson criterion;  $\Delta S$  is entropy of melting;  $R$  is gas constant;  $N_s$  and  $N_v$  are the number of an atom's nearest neighbors on the surface and within the body of a crystal. If  $\alpha$



is less than  $2 \text{ cal/}^\circ\text{C}$ , crystal grows isotropically with an atomically rough interface. By contrast, if  $\alpha$  is greater than 2, crystal is faceted with an atomically smooth surface. It is very interesting that for silicon the Jackson criterion for principal crystallographic planes varies in range from 0.89 for (110) plane to 1.87 for (100) plane, to 2.67 for (111) plane. Thus silicon crystal is a borderline material, of which the growth mode can easily change from faceted to non-faceted when the undercooling increases [63]. The variety in undercooling, which is induced by cooling rate during freezing or impurity element or others, will significantly cause the change in morphology of silicon either eutectic or primary. Generally speaking, for hypoeutectic or near eutectic DEASAs undercooling of  $5^\circ\text{C}$  is considered as a critical value to change the growth mode of silicon (Fig.18). Recently H.S.Kang et al [64] reported that the critical undercooling is a linear function of silicon content. For the higher silicon content an increased undercooling is required to change the morphology of eutectic silicon phase. They revealed that for Al-13%Si alloy at undercooling of  $14^\circ\text{C}$  the eutectic silicon morphology changes from flake to fibrous shape. However, for hypereutectic Al-20%Si alloy an increase in undercooling to  $73^\circ\text{C}$  is required. The different critical undercooling reported in literatures is thought to be associated with the different structure in liquid state. In current study DEASA melt is homogeneous, but the melt heating treated at  $720^\circ\text{C}$  in study by Kang is microheterogeneous, for which a deep undercooling /high cooling rate is needed to achieve the modified eutectic structure as evidenced in study[23].

Other important variety in structural feature of DEASAs is that iron-rich phase appears in fine flaky form instead of needle-like shape in the center of ingot containing iron concentration of 0.25% as shown in Fig.19. It is interesting that as Fe-level is more than 0.5% in EZL102 ingot the morphology of Fe-bearing precipitate also remain unchanged as shown in Fig.5. That is also attributed to effect of superheating the melt in electrolysis pot on the crystallization of iron-rich composition as reported in reference [33,34].



**Figure 19.** Fine flaky iron-rich phase indicated by arrow 2 appears in DEASA (EZL108) containing iron level of 0.25%.

### 3.2. Primary $\alpha$ -Al phase

Primary  $\alpha$ -Al phase is an important phase constituent, of which the volume fraction, grain size and morphology, dendrite arm space (DAS) and alloying element greatly affect the mechanical and foundry properties of hypoeutectic Al-Si alloys[65,66]. In DEASAs either eutectic such as EZL102, EZL108 and EZL109 or hypoeutectic such as EZL101, the volume proportion of primary  $\alpha$ -Al dendrite is higher than unmodified Al-7%Si alloy (ZL101) (Fig.20), and with increasing silicon content the volume percentage of Al-phase decreases. Undoubtedly, the increase of primary  $\alpha$ -Al dendrite greatly affects the properties of eutectic DEASA castings.

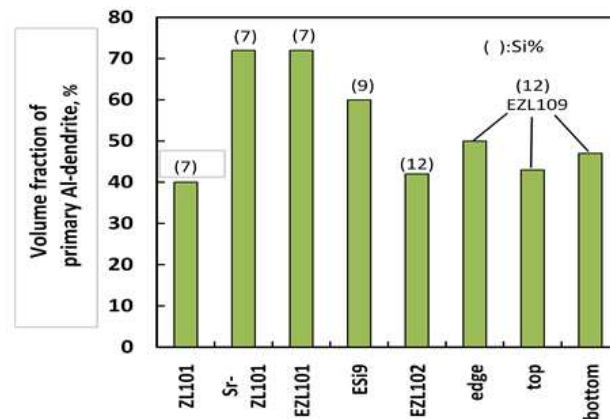


**Figure 20.** Volume fraction of  $\alpha$ -Al dendrite in commercial and electrolytic Al-Si alloys.

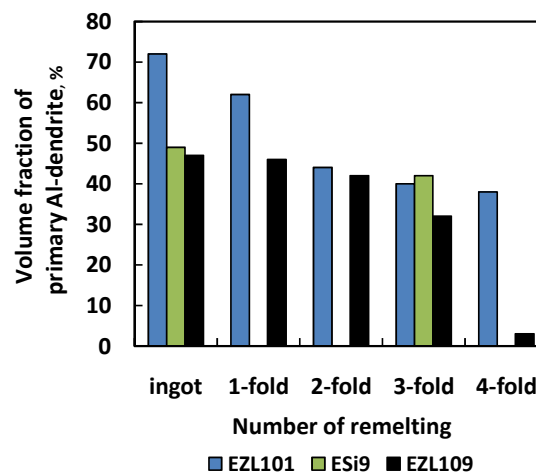


**Figure 21.** Volume percentage of  $\alpha$ -Al dendrite in DEASA against the remelting.

The volume percentage of  $\alpha$ -Al dendrite in the edge area of EZL109 ingot, where the cooling rate is much higher than bottom or top, is more or less larger than other areas (Fig.20). In addition, the volume proportion of aluminum dendrite decreases with remelting, which causes a decrease in undercooling in freezing (fig.18). After 3 or 4-fold remelting the volume percentage recovers to the value estimated from equilibrium Al-Si phase diagram (Fig.21) accompanying with an unmodified silicon structure. Apparently, the volume fraction of  $\alpha$ -



Al dendrite is a function of undercooling, which can be clarified using Al-Si quasi-diagram (Fig.3).

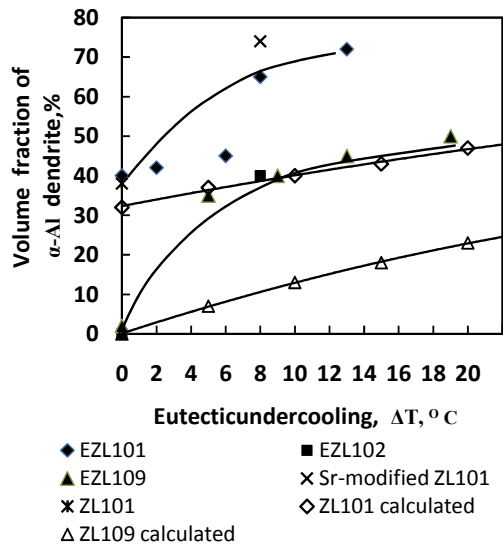


**Figure 22.** Volume percentage of  $\alpha$ -Al dendrite in DEASA is a function of undercooling in freezing.

The fact that undercooling shifts the eutectic content toward to higher level during freezing and depresses the eutectic temperature, leading to an increase in temperature interval, in which the primary aluminum phase precipitates from melt, and, thus, the volume fraction of Al-phase is increased. Curve EP (Fig.3) represents the relation between undercooling and silicon content solved in Al-matrix. Therefore, we are able to estimate the volume fraction of  $\alpha$ -Al dendrite in terms of undercooling in our tests (Fig.22). It is interesting that the volume fraction of  $\alpha$ -Al dendrite measured in our study is much higher than the value calculated in terms of curve EP. By combining the successful achievement of quasi-eutectic structure in EZL16 with undercooling of 9°C, which is much smaller than the critical undercooling of 20°C shown on curve ES to obtain quasi-eutectic for commercial Al-16Si alloy (Fig.3), it is reasonably postulated that the region of formation of quasi-eutectic structure in DEASA moves toward higher silicon content and smaller undercooling due to the homogeneous DEASA melt.

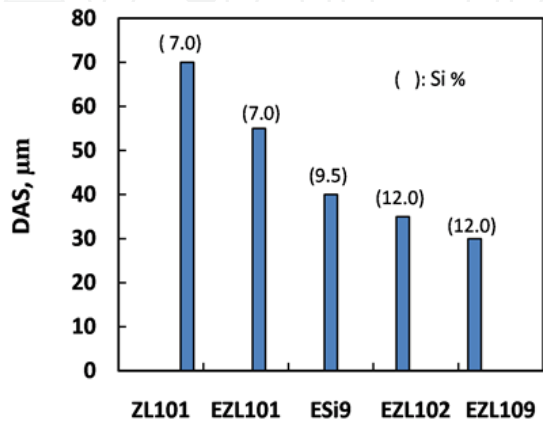


**Figure 23.** DAS of  $\alpha$ -Al dendrite in DEASA and commercial ZL101(A356) ingot .

Dendrite arm space (DAS) is an important crystallographic feature in primary Al-phase, greatly affecting the mechanical properties of hypoeutectic Al-Si alloys. The DAS, which is not related in any way to the volume percentage of Al-dendrite, can be varied considerably by cooling rate. As far back as the 1960s it has been found that for commercial Al-Si alloy castings with cooling rate in range of  $10^{-1}$ - $10^2$  °C/sec such as cast in sand and in a metal mould, and continuous castings the DAS value is a function of cooling rate as follows [67]:

$$d = A \cdot V^{-n} \quad (4)$$

where d is DAS ( $\mu\text{m}$ ), R is the cooling rate (°C/sec), A is related to the chemical composition and  $n=1/3$ - $1/2$ .

In electrolytic EZL101ingot having 7% Si content the primary Al-dendrite displays the smaller DAS value than commercial Sr-modified ZL101 ingot as seen in Fig.23. Meanwhile the DAS decreases with silicon content. After 2 or 3-fold remelting DAS value doesn't change, if any. That is related with the same cooling rate in freezing of those samples [67].

Summarizing the structural characteristics of DEASAs we reach the conclusion that the electrolytic alloy castings either hypoeutectic or eutectic or hypereutectic exhibit very fine eutectic silicon grain with high volume fraction of  $\alpha$ -Al dendrite, small DSA and small curved iron-bearing compound compared to commercial alloy. It is an advance superiority of DEASA over existing alloy for producing the high quality casting with excellent usage properties.

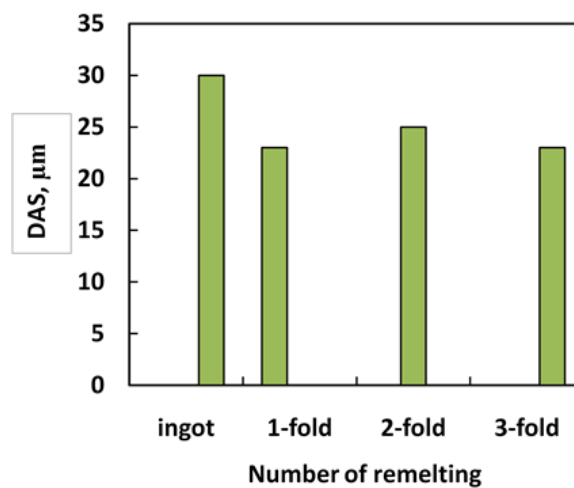


**Figure 24.** DAS in DEASA (EZL109) against remelting.

#### 4. Technological parameters influencing self-modification in DEASA castings

In foundry several technological parameters including amount of DEASA ingot in metallic charge, furnace temperature and holding time, remelting and level of modifier added into

melts, significantly affect the microstructure of castings and its mechanical properties. To optimize those parameters is an important event for producing high quality cast product with low cost.

In this chapter we have discussed the structural heredity of alloys upon remelting. It is concluded that remelting a fine metal easily produced a fine casting compared to a coarse metal at the same condition [68]. Experimental results demonstrated that at least 10% of a fine Al-Si ingot is required to achieve a casting with fine silicon grain [69]. Therefore, amount of DEASA ingot added in metal charge is an important factor for producing a casting with the fully modified microstructure.

In our test the metallic charge is composed of EZL101 ingot (Table 1.), pure aluminum ingot and Al-20%Si along with other master alloy additions. No modifier is added in melt. The percentage of DEASA ingot in metallic charge ranges from 10 to 50%. Table 3. lists the chemical analysis of alloys tested. Note that with either the holding time in furnace or remelting the strontium content is unchanged and much less than the critical level (0.004%) to create a modified eutectic in Al-Si alloys [70, 71]. Thus, the change in microstructure is associated with the amount of DEASA ingot used rather than strontium content in alloy.

| Alloy   | Amount of DEASA (%) | Number of remelting | Holding time (min) | Chemical Analysis wt% |      |       |      |       |       |       |       |        |
|---------|---------------------|---------------------|--------------------|-----------------------|------|-------|------|-------|-------|-------|-------|--------|
|         |                     |                     |                    | Si                    | Mg   | Ti    | Fe   | Cu    | Mn    | Zn    | Ni    | Sr     |
| EA50-0* | 50                  | 0                   | 10                 | 7.33                  | 0.21 | 0.11  | 0.21 | <0.01 | 0.01  | 0.003 | 0.016 | 0.0011 |
| EA30-0  | 30                  | 0                   | 10                 | 7.08                  | 0.41 | 0.19  | 0.27 | <0.01 | 0.006 | 0.012 | 0.007 | 0.0012 |
|         |                     |                     | 120                | 6.90                  | 0.34 | 0.17  | 0.30 | <0.01 | 0.007 | 0.012 | 0.006 | 0.0013 |
|         |                     |                     | 240                | 6.98                  | 0.30 | 0.17  | 0.25 | <0.01 | 0.007 | 0.012 | 0.006 | 0.0012 |
| EA30-2  |                     | 2                   | 120                | 7.00                  | 0.25 | 0.21  | 0.26 | <0.01 | 0.006 | 0.012 | 0.009 | 0.0011 |
| EA10-0  | 10                  | 0                   | 10                 | 6.71                  | 0.39 | 0.053 | 0.25 | <0.01 | 0.009 | 0.015 | 0.038 | 0.0016 |
|         |                     |                     | 120                | 6.84                  | 0.28 | 0.050 | 0.25 | <0.01 | 0.009 | 0.015 | 0.006 | 0.0016 |
|         |                     |                     | 240                | 6.50                  | 0.28 | 0.048 | 0.25 | <0.01 | 0.009 | 0.015 | 0.006 | 0.0014 |
| EA10-2  |                     | 2                   | 10                 | 6.69                  | 0.32 | 0.047 | 0.26 | <0.01 | 0.006 | 0.013 | -     | 0.0012 |

E: electrolytic; A: Al-Si alloy; 50: 50% of DEASA in charge; 0: no remelting.

**Table 3.** Technological parameters and chemical analysis of DEASA alloys wt%

When 10% of metallic charge is DEASA silicon crystals grow in modified manner in as-cast microstructure of EA10-0 alloy, but a few silicon flakes can be found (Fig.25). However, increasing the amount of DEASA to 30% (EA30-0) or more (EA50-0) results in a fully

modified microstructure as seen in Fig.26. It would be expected that the self-modified silicon crystal in DEASA acts as a modifier for the commercial Al-Si alloy. Like Na, Sr and other modifiers there is a critical amount of DEASA, below which the eutectic is not modifiable. For ZL101(A356) alloy 30% DEASA ingot in metallic charge is needed to obtain a full modified microstructure. Obviously, the higher the amount of DEASA used in charge, the stronger the trend to modification in alloy. Note that there is no overmodification with increasing the amount of DEASA ingot. It is a superior characteristic of DEASA castings to existing Al-Si alloy.

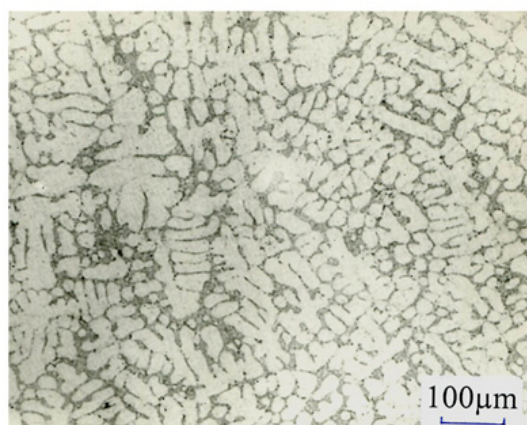


**Figure 25.** Modified microstructure of EA10-0 alloy with 10% of DEASA ingot in metallic charge and holding time of 10min.. Some silicon flake can be found. Optical

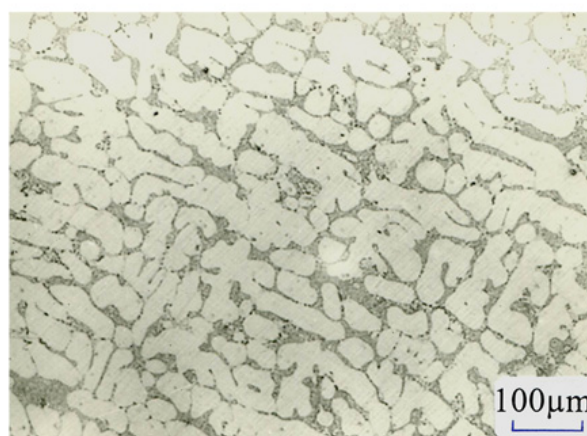


**Figure 26.** Optical microstructure of EA30-0 alloy with 30% of DEASA ingot in metallic charge and holding time of 10min, indicating a completely modified eutectic silicon..

Self-modified structure in EZL101(A356) alloys with either 10% or 30% of DEASA (EA10-0 and EA30-0) ingot strongly depends upon remelting and furnace holding time. When furnace holding time at 720°C is about 120min, both EA10-0 and EA30-0 alloys are subjected

to partial structural fading as shown in Figs.27 and 28. Our test results reveal that for both alloys the inheritance of modified structure can be survived after first remelting. However, upon 2-fold remelting EA10-2 with 10% DEASA is subjected to partially fading in modified structure (Fig.29). As amount of DEASA increases to 30% (EA30-2), the modified structure can be maintained upon 2-fold remelting with holding time of 2 hrs, as shown in Fig.30, but when the holding time excesses 2 hours, some silicon flakes can be found.

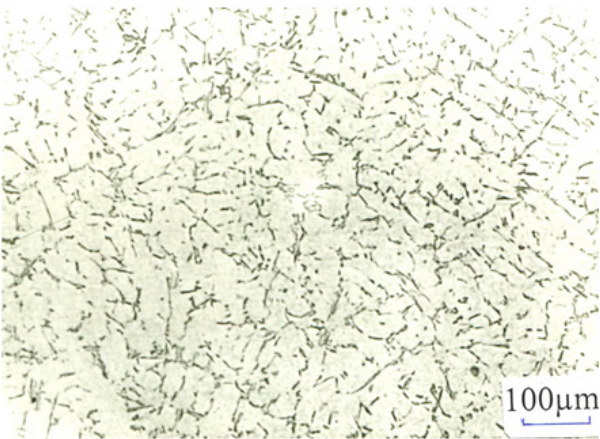


**Figure 27.** Optical micrograph of EA10-2 with 10% of DEASA ingot and holding time of 2hr at 720°C, indicating the unmodified structure.

In general, in foundries casting must be done within two hours after degassing aluminum melts in furnace. It is evident that strengthening the modification of DEASA alloys is needed for producing high quality castings. Below we will discuss the effect of small amount of strontium added into the molten alloy on the modified structure after different holding time. Table 4. lists the chemical analysis of Sr-modified DEASAs in tests.

| Alloy  | Amount of DEASA.% | Holding time. min | Chemical Analysis wt% |      |       |       |      |       |       |       |       |       |
|--------|-------------------|-------------------|-----------------------|------|-------|-------|------|-------|-------|-------|-------|-------|
|        |                   |                   | Si                    | Mg   | Cu    | Mn    | Fe   | Ti    | Cr    | Ni    | Zn    | Sr    |
| SEA10* | 10%               | 10                | 7.08                  | 0.43 | 0.03  | 0.006 | 0.29 | 0.064 | <0.00 | —     | 0.014 | 0.003 |
|        |                   | 120               | 6.84                  | 0.28 | 0.04  | 0.009 | 0.35 | 0.088 | 0.004 | 0.006 | 0.015 | 0.002 |
|        |                   | 240               | 6.95                  | 0.30 | 0.04  | 0.015 | 0.33 | 0.070 | 0.004 | 0.008 | 0.017 | 0.002 |
| SEA30  | 30%               | 10                | 6.81                  | 0.39 | 0.032 | 0.007 | 0.36 | 0.16  | 0.002 | 0.004 | 0.012 | 0.003 |
|        |                   | 120               | 6.66                  | 0.34 | 0.032 | 0.007 | 0.35 | 0.17  | 0.002 | 0.006 | 0.012 | 0.002 |
|        |                   | 240               | 6.50                  | 0.32 | 0.033 | 0.007 | 0.35 | 0.17  | 0.002 | 0.003 | 0.012 | 0.002 |

\*S: Sr-modification; E: electrolytic; A: Al-Si alloy; 10: 10% of DEASA in charge.

**Table 4.** Chemical analysis of EZL101 alloys tested



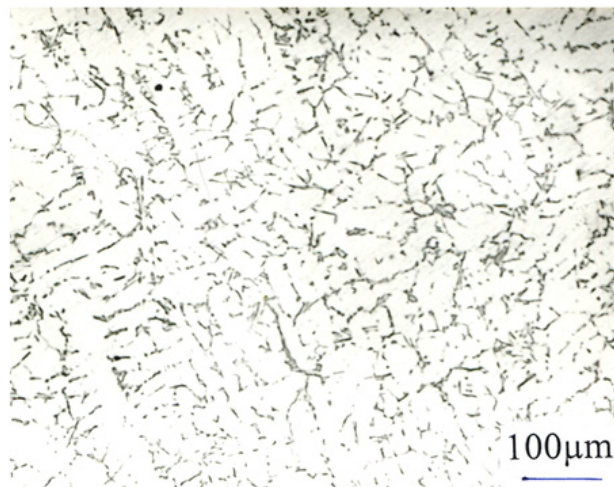


**Figure 28.** Micrograph of EA30-2 with 30% of DEASA ingot and holding time of 2hr at 720°C, indicating the unmodified structure. Optical

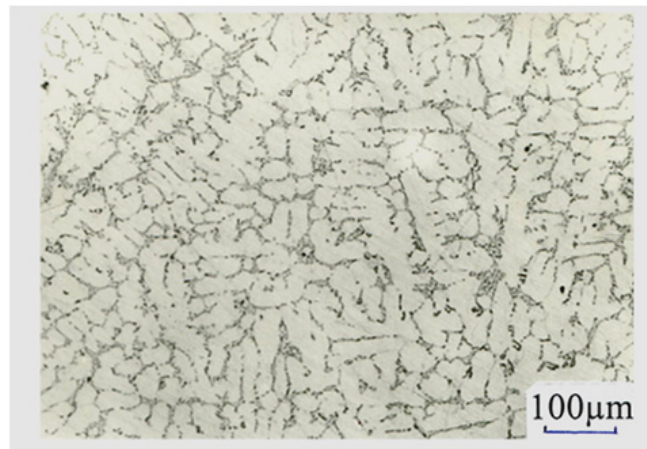


**Figure 29.** Optical micrograph of EA10-2 with 10% of DEASA ingot upon 2-fold remelting, indicating the partial fading of modified structure.

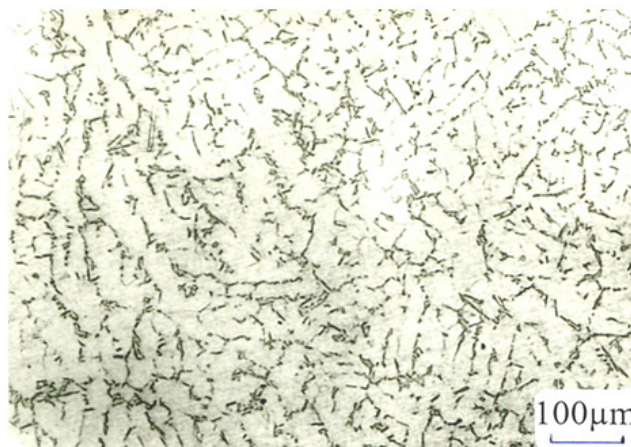


**Figure 30.** Micrograph of EA30-2 with 30% of DEASA ingot upon 2-fold remelting and holding time of 2 hrs, showing the modified structure. Optical.



Note that after adding Al-10%Sr master alloy into melts the level of Sr in alloys increases to about 0.003%, which is less than in commercial Sr-modified alloys, resulting in a fully modified structure in either SEA10 or SEA30 alloy (Fig.31). It is important that when holding time is four hours, in microstructure of SEA10 alloy some flaky silicon crystal can be found, but for SEA30 alloy the modification fading occurs in some degree as seen in Fig.32. Later is sufficient to meet the requirement in foundry. 30% of DEASA used in charge with 0.002-0.003% of Sr-level in alloy are necessary to produce high-quality Al-Si alloy. The process, in which the low level of strontium addition promotes a fully modified structure, is an advance advantage of DEASAs over Sr- or Na-modified Al-Si alloys.

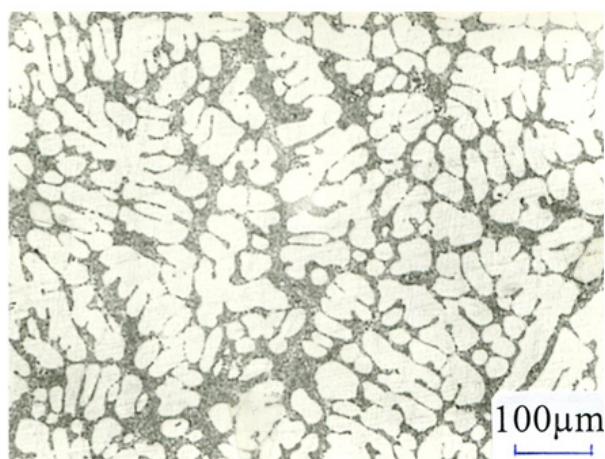


**Figure 31.** Micrograph of SEA30 alloy after furnace holding of 10min, showing the modified structure Optical.

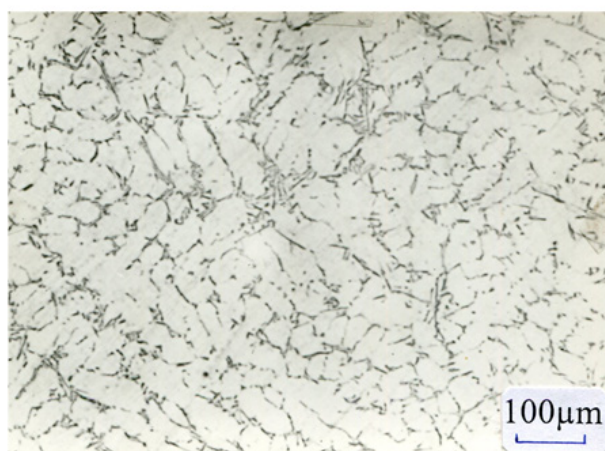


**Figure 32.** Partial modified microstructure of SEA30 alloy after furnace holding of 4hr at 720°C. Optical

## 5. High-quality automotive wheels made from DEASA

The wheel is an important part of a vehicle in terms of safety. The impact strength and fatigue life are on the top of the quality list of wheel characteristics. Al-7Si-0.3Mg alloy(A356), due to higher impact resistance and fatigue life, good castability and

machinability, is a preferred choice to produce quality wheel. A lot of studies have demonstrated that the mechanical properties of A356 alloys are strongly affected by morphologies of eutectic silicon, iron content and porosity dispersed in castings, which is associated with the impurity modification and hydrogen level [71, 72]. For producing the quality wheel with higher impact resistance the maximum allowable iron level is limited to 0.20%. As mentioned above, DEASAs exhibit the excellent modified structure with a low level of modifier such as Sr, accompanying with the stringy Fe-rich precipitate of small size (Fig.19). Thus, the wheel made from DEASAs might be porous-free, resulting in higher impact resistance, ductility and tensile strength. At the end of last century we have examined the mechanical properties of wheel made from DEASA ingot (ES9, Tab.1) in the foundry [14].

A 600kg crucible was used to prepare the melts in an electric furnace. The metallic charge consisted of pure aluminum ingot, clean scrap of A356 alloy, other master alloy and DEASA (ES9) ingot pieces, of which the amount was a third of charge. Each melt was degassed with N<sub>2</sub> at temperature of 710°C. After degassing and holding for 15min, a small amount of Al-10%Sr master alloy was added into the melt to obtain Sr level in alloy below the critical value of 0.003%. Then the prepared melts were poured into a permanent mold to produce wheel casting and Y-shape plate castings with dimension of 22×150×220mm<sup>3</sup>. Finally, the castings were heat treated to a T<sub>6</sub> temper by solution at 535°C for 4 hrs, water quenching, and aging at 135°C for 6 hours. Table 5. lists the chemical analysis of DEASA (ES9) and EZL101 alloys, which have the different iron level, near or above the allowable value of 0.20% for wheel casting in order to clarify the effect of Fe-rich precipitate on the mechanical properties of DEASA wheels.

| Alloy       | Si        | Mg        | Ti        | Fe        | Cu    | Mn    | Zn   | Sr            | RE     |
|-------------|-----------|-----------|-----------|-----------|-------|-------|------|---------------|--------|
| E S9        | 9.20-9.60 | <0.01     | 0.40-0.60 | 0.44-0.65 | <0.02 | 0.005 | 0.03 | 0.001-0.004   | 0.03   |
| EZL101-17   | 6.63-6.80 | 0.28-0.30 | 0.12      | 0.16-0.17 | 0.03  | 0.1   | 0.01 | 0.0016-0.0024 | —      |
| EZL101-21   | 6.50-7.00 | 0.24-0.27 | 0.10      | 0.19-0.22 | 0.03  | 0.01  | 0.01 | 0.0022-0.0030 | —      |
| EZL101-27   | 6.90-7.30 | 0.28-0.30 | 0.10      | 0.26-0.27 | 0.03  | 0.008 | 0.01 | 0.0031-0.0034 | —      |
| ZL101(A356) | 6.90      | 0.30      | 0.12      | 0.10-0.13 | 0.02  | 0.01  | 0.01 | 0.0060-0.0080 | 0.0005 |

**Table 5.** Chemical analysis of DEASAs for wheel tested wt%

Table 6. lists the mechanical properties of conventional (ZL101A) and electrolytic Al-7Si-Mg alloy (EZL101). As iron content is less than or near the maximum allowable limit of 0.20%, the superiority of DEASAs over existing alloy is very evident. DEASA alloys offer the mechanical properties higher than existing alloy (ZL101A) with lower iron content of 0.12%. As increasing Fe-level from 0.21 to 0.27% there is a slight tendency to decrease the

mechanical indexes. But the tensile strength remains to be higher than conventional alloy (ZL101A), the elongation and impact strength are lower than existing alloy.

| Alloy  | Fe content wt% | Tensile strength MPa | Elongation % | Impact strength J/cm <sup>2</sup> | Hardness HB |
|--------|----------------|----------------------|--------------|-----------------------------------|-------------|
| ZL101A | 0.12           | (213-238)/225        | (7-16)/12    | (15-52)/32                        | (76-80)/78  |
| EZL101 | 0.16           | (217-260)/239        | (7-18)/13    | (31-52)/37                        | (74-80)/76  |
|        | 0.21           | (211-241)/231        | (11-20)/14   | (28-52)/38                        | (75-85)/79  |
|        | 0.27           | (218-240)/232        | (7-10)/8     | (16-52)/29                        | (70-85)/79  |

Note: ①Test samples are cut from Y-shape plate castings with dimension of 22x150x220mm<sup>3</sup>

②(Range of data)/Average data.

③Averaged data obtained from 4 Y-shape plate castings poured after holding time of 10 and 90min in furnace, respectively.

**Table 6.** Mechanical properties of conventional and electrolytic Al-Si alloys with different Fe-level

Wheel impact strength test is carried out at wheel shock testing apparatus (Fig.33). In general, the critical impact strength for automobile wheel is 230mm (height) ×6000kN (weight) at 13degree of inclination. In production some 50% of the wheels made from ZL101 (A356) alloy exceed this minimum requirement by 10-20%. Addition of DEASA in charge exerts a significant improvement on the shock resistance. Testing results demonstrate that the wheels made of DEASA with different iron level offer the impact value exceeding 256mm×6000kN at 13degree of inclination, and most of them are higher than 276mm×6000kN, which exceeds the critical requirement by 20%. Moreover, in the extreme test at 30 degree of declination two third of DEASA wheels tested exceed the shock resistance of 230mm×1010kN. However, none of wheel made from ZL101(A356) could pass this limit.

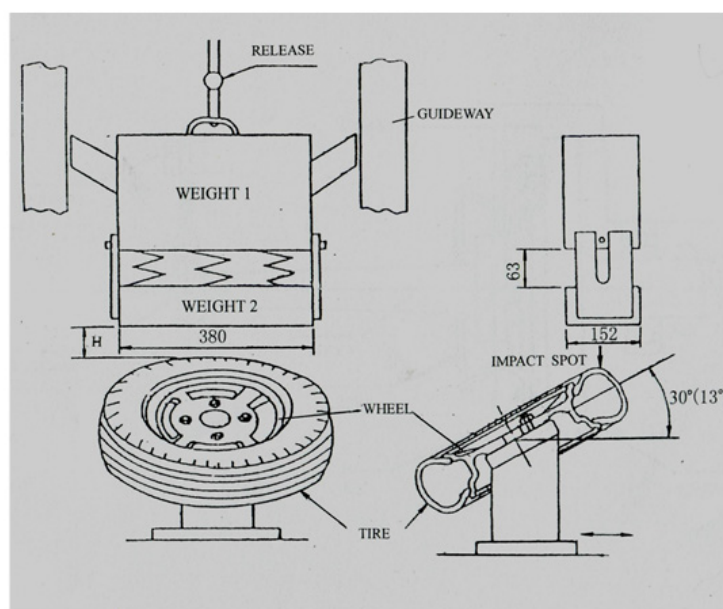


**Figure 33.** Schematic drawing of wheel shock testing apparatus

Fig.34 shows the wheel fatigue test apparatus, which uses torque of 3000N-M for loading with rotating speed of 1500rpm of shift. For wheel of 14 or 15 inches diameter the design fatigue lifetime, which is expressed in terms of the number of cycles-to-failure, is  $10^5$  cycles. Usually the lifetime for wheel made of ZL101(A356) ranges from  $0.4$  to  $2.0 \times 10^5$  cycles. Some of them are not capable of exceeding the minimum lifetime. However, experimental data show that the dramatic improvement in impact resistance on DEASAs stated above is also evident in fatigue strength. DEASA wheels with iron content exceeding the allowable limit of 0.20% exhibit higher fatigue lifetime exceeding  $2.0 \times 10^5$  cycles, except for E356-27 with higher iron content of 0.27% that has fatigue lifetime of  $1.5 \times 10^5$  cycles.

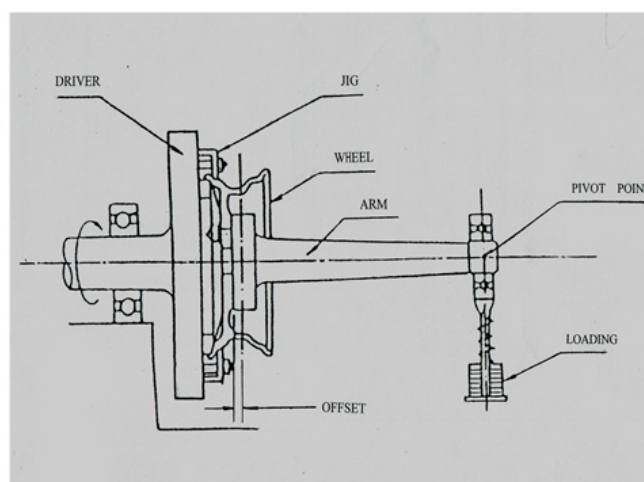


**Figure 34.** Schematic diagram of wheel fatigue testing apparatus

Summarizing the experimental results it is reasonable to conclude that as iron content exceeds the maximum allowable limit of iron level of 0.20% in some degree, for example, reaching 0.27%, the mechanical properties of DEASAs, especially impact strength and fatigue resistance, significantly are improved. Therefore, it is expected that the allowable iron content would be limited to more than 0.20%, which would save the cost of wheel.

The reason why DEASA wheel containing different iron level exhibits an excellent impact strength and fatigue resistance compared to conventional alloy, is believed to be attributed to porosity, if the difference between morphologies of silicon crystals and Al-dendrites in DEASA and existing A356 is difficult to find in micrography of the wheel as demonstrated in Fig.35 and 36. Porosity is an undesirable feature of the cast structure because pores, either surface or internal, acting as stress raiser during loading, seriously degrade the mechanical properties [73-75]. This inference is strongly supported by leak test for wheel, revealing that all the DEASA wheels were leakproof, while 10% of ZL101 (A356) wheels were not. Moreover, visual inspection showed that no pinholes and microporosities could be found on the surface of DEASA wheels compared to common ZL101, implying that DEASA wheels exhibit much less porosity than existing alloy. Undoubtedly, the sound alloy made from DEASA has higher mechanical properties.



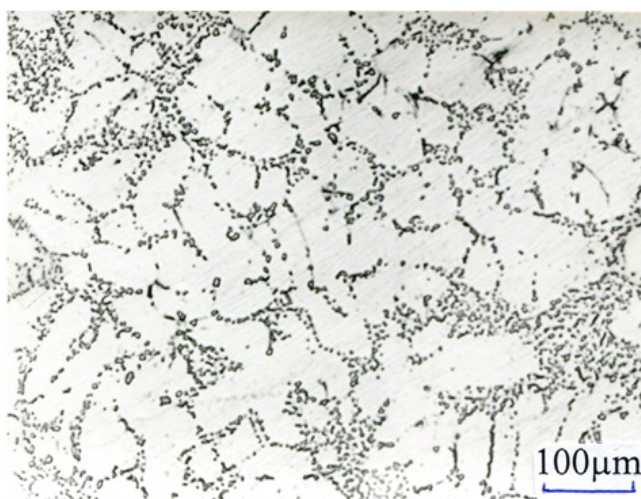


**Figure 35.** Optical microstructure of hub in wheel made from DEASA EZL101-17 (Table 6.) heat-treated by T<sub>6</sub>

The origin of porosity is associated with two important, if not primary important, factors for Al-Si alloy in given casting condition, i.e. hydrogen dissolved in melt and amount of strontium or sodium added in molten alloy as modifier [71,76,77]. High hydrogen level causes an increase in porosity, resulting in decrease in mechanical properties [72-75]. Strontium or sodium increases the tendency to porosity of alloy [71]. In our study due to self-modification in DEASA ingot much less amount of modifier is required to be added into the DEASA molten alloy. Therefore, the tendency to porosity becomes weakened and sound castings are more easily obtained, resulting in higher impact resistance and fatigue strength in DEASA wheel.

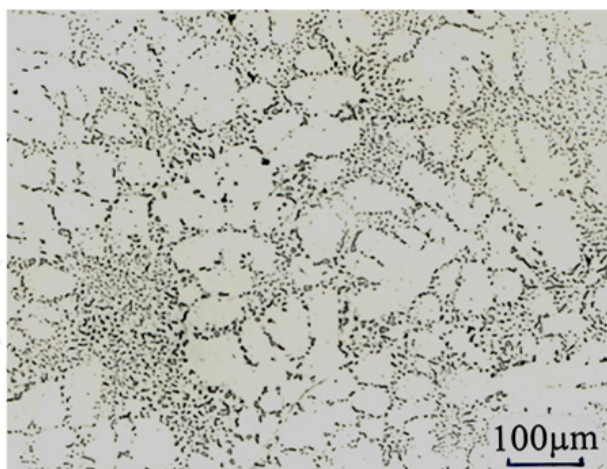


**Figure 36.** Microstructure of hub in wheel made of commercial A356 alloy heat treated by T<sub>6</sub> Optical

Until now a few studies have been done on the behavior of hydrogen in aluminum in electrolytic process [78]. In electrolytic pot the surface of aluminum melt is usually crusted over by fused cryolite, acting as an insulator to isolate the liquid from the atmosphere and protecting melt from hydrogen pick-up. In this case the hydrogen level is very low. Prodhan [47] studied the behavior of hydrogen in Al-Si alloy during solidification under electric field,

indicating that the hydrogen level can be decreased from 2.5ppm to 1.7ppm. This is within the acceptable limit of pore-free castings [47]. It would be expected that in electrolytic process the hydrogen in Al-Si alloy melt can be removed under electric field. Undoubtedly, the decreased hydrogen level in DEASAs strongly weakens the trend to porosity, enhancing the impact resistance and fatigue strength. It is evident that the electrolytic process would be a powerful mean to reduce the hydrogen level in alloy.

## 6. Conclusion

1. DEASAs either hypoeutectic or eutectic display self-modified structure in ingot with excellent structural inheritance upon remelting. DEASA is self-undercooled alloy.
2. Hypereutectic DEASAs with silicon in range from 13% to 17% exhibit completely self-modified eutectic structure, but are subjected to fully fading upon remelting due to disappearance of undercooling in freezing.
3. DEASAs have high volume of  $\alpha$ -Al dendrite that is associated with the high undercooling in freezing.
4. DEASAs are insensitive to cooling rate in freezing.
5. Iron-bearing precipitate in DEASAs appears in small curved shape as iron level increases to near 0.5%.
6. 30% DEASA ingot in metallic charge with added Sr-level of 0.002-0.003% is necessary to produce high quality Al-Si casting with self-modified structure.
7. Automobile wheel made of DEASA display high impact resistance and fracture strength that is associated to small amount of Sr-modifier added into melt, low hydrogen concentration and small curved shape of iron-rich compound.
8. Electrolysis is a potential measure to produce high quality Al-Si casting.

## Author details

Ruyao Wang and Weihua Lu

*Institute of Material Science and Engineering, Donghua University,  
Shanghai, P.R.China*

## 7. References

- [1] Hayward C.R( 1955) An Outline of Metallurgical Practice. Third Edition. Toronto: D.Van Nostrand Company, Inc.285-286p.
- [2] Frilley J (1911) Revue de Metallurgie. j. 8(7): 518-523
- [3] Bullough V.L (1973) US Patent No.3 765 878 Oct.16.
- [4] Qiu Z.X, Zhang Z.L, Grjotheim K, Kvande H (1987) Aluminium.j. 6312:1247-1250.
- [5] Orman Z (1976) Rudy Met. Niezelez. j. 21(5): 162-164.
- [6] Weslan D (1984) US Patent No.4 425 308. Jan.10, 1984.
- [7] Keller R, Weld B.J, Tabereau A.T (1990) In: Light metals 1990. TMS. pp.333-340.



- [8] Moxnes B, Gikling H, Kvande H, Rolseth S, Straumsheim K(2003) In: Crepeau P , editor. Light Metals 2003. TMS. pp.329-334.
- [9] Tabereaux A.T, McMin C.J(1978) In: Light Metals 1978 .TMS.pp.209-222.
- [10] McMin C. J, Tabereaux A.T (1976) US Patent No 3 980 537 Sept.14, 1976.
- [11] Yang K.Q, Gu Q.S, Tian G.Y, Li Q.C(1994) Chinese Patent. ZL94 11 6235.4, March 4<sup>th</sup> 1994.(In Chinese)
- [12] Yang K.Q, Yang S (1997) Foundry. j. No.1: 44-46. (In Chinese)
- [13] Yang D.X.,Wang R.Y(1994) Hot Working Technology. j. No.2: 19-21.(In Chinese)
- [14] Wang R.Y, Lu W.H (2001) Light Metal Age. j. 59(5/6):.6-10.
- [15] Wang R.Y.,Lu W.H ,Hogan L.M (2003) Mat.Sci.Eng. j.A348: 289-298.
- [16] Bloomfield L.A, Freeman R.R, Brown W.L (1954) Phys. Rev. Letter. j. 54:2246-2249.
- [17] Mitsuo S (1997) Liquid Metals. London: Academic Press. pp.41, 235-236.
- [18] Iida T, Guthrie R.I.L (1988) The Physical Properties of Liquid Metals. Oxford: Clarendon Press. pp.18-46.
- [19] Gui M.C, Li Q.C, Jun J(1995) Special Casting and Nonferrous Alloys.j.15(1):5-8.(In Chinese)
- [20] Eskin D.G (1996) Z. Metallkunde.j. 89(4):295-301.
- [21] Popel P.S, Tchikova O.A., Brodova J.G, Makeev V.V (1992) Nonferrous Metals. J. No.9: 53-56(In Russian).
- [22] Bian X.F, Wang W.M (2000) Materials letters .j. 44(1): 54-58.
- [23] Brodova J.G, Popel P.S.,Eskin G.I (2002) Liquid Metal Processing. Application to Aluminum Alloy Production. London: Taylor and Francis. pp.85-145.
- [24] Wang, L.D. Zhu D.Y, Wei Z.I, Chen Y.L, Huang L.G, Li Q.J, Wang Y.S (2011) Advance of Materials Research. J.146-147:79-89.
- [25] Nikitin V.I (1991) Foundry Production.j. No.4:4-5(In Russian)
- [26] Li P.J,. Xiong Y.H, Zhang Y.F, Zeng D.B(2003) Trans.Nonferrous Met. Soc.China.j. 13 (2):.329-334.
- [27] Singh M. Kumar R (1973) J. Mater. Sci. j. 8: 317-323.
- [28] Zhang L.,Bian X.F, Ma J.J(1995) Foundry. j. No.10:7-12(In Chinese).
- [29] Wang W.M, Bian X.F, Wang H.R, Wang Z, Lin Z.G, Liu J.M(2001) J. Materials Research. J. 16(12): 592-3598.
- [30] Xu C.L, Jing Q.C(2006) Mat.Sci.Eng.j. A437 (2): 451-455
- [31] Gui M.C, Li Q.C, Jia J(1995) Special Casting and Nonferrous Alloys. j. 15 (1):.5-8 (In Chinese)
- [32] Zhang R.,Zhang L.M, Yang Z.H, Liu L(2011) Materials Sci. Forum. J. 654-656:.1412-1415.
- [33] Ri E.K, Ri K.S, Khimukhin S.N, Kalugin M.Y, Statsenko D.P, Kryuchkov I.V (2011) Foundry Production .j. No.7: 10-12 (In Russian).
- [34] Awano Y, Shimizu Y (1987) Imono.J.59(4): 233-238; 59(7):.415-420 (In Japanese).
- [35] Li P.J,Nikitin V.I, Kandalova E.G, Nikitin K.V(2002) Mater.Sci.Eng.j.A332:371-372.
- [36] Müller K(1998) Metall. J.52 (1-2):29-35.
- [37] Gubinko A.Y (1991)Foundry Production. No.4: 19-20 (In Russian).

- [38] Zhao Z.L, Wang J.L, Lu L (2011) *Materials and Manufacturing Processing*.j. 26(2):249-254.
- [39] Prodhan A, Sanyal D (1998) *Materials Science Letter*.j. 16(11):.958-961.
- [40] Prodhan A, Sivaramakrishnan C.S, Chakrabarti A. K.(2001)*Met Mat. Trans B*. j.32(2):.372-3780.
- [41] Yu S.R.,Zheng Y.H, Feng H, Cai L.G(2010) *Hot working technology*.j.39(9):47-50 (In Chinese).
- [42] Conral H (2000) *Mat. Sci. Eng. J.A287*(8): 205-212.
- [43] Li H, Bian X.F, Liu X.F, Ma J.J (1996) *Special Casting and Nonferrous Alloys*. J.16(3): 8-10 (In Chinese).
- [44] Huang L.G, Gao Z.Y, Zhang Z.M (2009) *Foundry Technology*.j.30(5):650-652 (In Chinese).
- [45] Temchenko S.L, Zadoroschnai N.A (2005) *Foundry Production*.j. No.9: 12-13.(In Russian)
- [46] B.A.Rabkin, S.L.Temchenko(2003) *Foundry Production*.j.No.10:.17-19(In Russian).
- [47] Prodhan A (2009) *AFS Trans*. J.117: 63-77
- [48] Loper C.R, Lu D.Y, Kang C.S (1985) *AFS Trans*. j. 93:533-543.
- [49] Wang R.Y, Lu W.H (2007) *AFS Trans*. J.115: 241-248.
- [50] Thall B.M, Chalmer B (1950) *J.Inst. Metals*. j. 77:79-97.
- [51] Kim C. B, Heine R.W (1963-1964) *J. Inst. Met*. j. 92:367-376.
- [52] Jenkinson D.C, Hogan L.M (1975) *J. Crystal Growth*. j. 28:171-187.
- [53] Fredriksson H (1991) *Scand. J. Metallurgy*.J.20: 43-49.
- [54] Talaat El-Benawy, Fredriksson H (2000) *Trans. J. of Japanese Institute of Light Metals*. j. 41:507-515.
- [55] Stuhldreier G, Stoffregen K.W (1981) *Giesserei*. j. 68: 404-409.
- [56] Stoffregen K.W (1985) *Giesserei*.j. 72: 545-549.
- [57] Mondolfo L.F(1979) *Aluminum Alloys, Structures and Properties*.London: Butterworths.pp.513-515; 534-537; 566-575;592-594;604;614-615;617-618.
- [58] Apelian D, K.Sigworth G, Whaler K.R (1984) *AFS Trans*.j. 92: 297-370.
- [59] Wang R.Y, Lu W.H.Hogan L.M (1995) *Mat. Sci.Tec*. j. 11(5):.441-449.
- [60] Wang R.Y, Lu W.H, Hogan L.M(1999) *J. Crystal Growth* .j. 207:43-54 .
- [61] Wang R.Y, Lu W.H, Hogan L.M(1997) *Trans. Metall. Mater*.j.28A:1233-1243.
- [62] Jackson K.A(1958) *Mechnism of growth*, In: *Liquid Metals and Solidification*, ASM, Cleveland, OH.pp.174-186.
- [63] Gilmer G.H.,Leaming H.J.,Jackson K.A (1974) *Liquid Metals and Solidification*. Proc.4<sup>th</sup> Int. Conf. on Crystal Growth, Amsterdam, North-holland. pp.495.
- [64] Kang H.S.,Yoon W.Y.,Kim K.H, Kim M.H. Yoon E.P(2004) *Mater. Sci. Forum*. j. 449-452: 169-172.
- [65] Oswalt K.J, Misra M.S(1980) *AFS Trans*. J. 88: 845-862.
- [66] Mi J.W , Cheng J.N.,Yu Y.M (1990) In: C.Q.Chen, F.A.Starke.editors. *Proceedings of the second international conference on aluminum alloys*. Beijing: pp.566-570.

- [67] Dobatkin V.I, Eskin G.I.(1990) In: C.Q.Chen, F.A.Starke.editors. Proceedings of the second international conference on aluminum alloys. Beijing: pp278-282
- [68] Li S.S, Zhu Y.F, Zeng D.B (1999) Foundry. j. No.8:53-58 (In Chinese).
- [69] Lui X.F, Bian X.F,.Ma J.J et al(1994) Foundry.j. No.10:18-23 (In Chinese)
- [70] Lu W.H., Wang R.Y(1995) Special Casting and Nonferrous Alloys.j.15(2):1-5. (In Chinese).
- [71] Gruzleski J.E., Closset B.M (1990) The Treatment of Liquid Aluminum-Silicon Alloys. AFS Inc. Des Plaines, IL, US. pp.223; chapter 4.
- [72] Anyalebechi P.N(2003) In: P N. Crepeau. Editor. Light Metals 2003. TMS. pp.971-981.
- [73] Eady J.A,.Smith D.M (1986) Materials Forum.j. 9(4):.217-223.
- [74] Surappa M.K, Blank E.J, Jacquet.C (1986) Script Metallurgica.j. 20(9):.1281-1286.
- [75] Caceeres C.H (1995) Script Metallurgica et Materialia.j. 32(11):1851-1886.
- [76] Mascre C, Lefebvre M (1959) Fonderie. j. No.166:484-497.
- [77] Arbenz H(1962) Giesserei.j. 49:105-110.
- [78] Zhang M.J, Qiu Z.X, Di H.L (1987) Nonferrous Metals. No.1:27-31;No.2:29-34 (In Chinese).